Modeling Segregation and Grain Structure Development in Equiaxed Solidification with Convection

C. Beckermann

Modeling the development of micro- and macrosegregation patterns and grain structures in the equiaxed solidification of metal alloys under the combined influences of melt convection and the motion of free solid has been the subject of intense recent research efforts. This article presents a summary of selected experimental and theoretical studies aimed at understanding the convective transport processes both for a single grain and at the scale of a casting. The need for much additional research is emphasized.

INTRODUCTION

The as-solidified structure of most statically and continuously cast metal alloys features both columnar (long, aligned) and equiaxed (spheroidal) grains. This is true for steels as well as aluminum alloys. A fine equiaxed grain structure is often preferred over a columnar structure for a number of reasons (single-crystal turbine blades are an important exception):[1] uniform mechanical properties and better overall strength and fatigue life, more finely dispersed second phases and porosity, less macrosegregation, improved feeding to compensate for shrinkage and less hot cracking, improved surface properties, and improved machinability and fabricability.

An equiaxed grain structure can be promoted by the enhancement of heterogeneous nucleation in the bulk melt through the use of grain refiners (such as TiB_2 in aluminum alloys) and the fragmentation of existing dendrites at the junction between a branch and its stem.
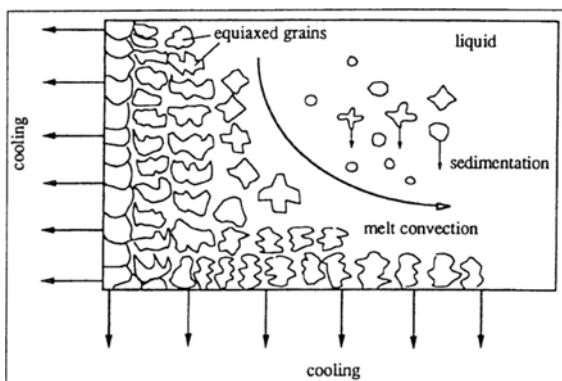
In the latter mechanism, melt flow is necessary to transport the fragments into the interior bulk liquid where they may survive and grow into equiaxed crystals. The beneficial influences of increased superheat, alloying content, mold vibration, mold rotation, and electromagnetic or mechanical stirring can all be linked to fragmentation.

These effects have been understood on a qualitative level for decades, but the prediction of the resulting state and size distribution of grains, phases, and species in the solidified metals has been complicated by the intricate physical phenomena involved. This article summarizes recent advances in modeling solute redistribution and grain structure formation in purely equiaxed alloy solidification (Figure 1); the emphasis is on the influence of convection. Columnar growth and other grain structures are not considered.

BASIC MODELING CONSIDERATIONS

It was not until recently that microstructural evolution models were linked to macroscale heat-flow calculations to predict structural and compositional features at the scale of a cast part.[2,3] Most of the existing work in the area of micro- and macroscopic modeling has only considered the diffusion of solutes (at the scale of the grain) and heat (at the scale of the casting), while neglecting any melt convection and transport of fragments and unattached equiaxed grains.

In a purely diffusive environment, the equiaxed grains are thought to nucleate in the melt and remain stationary during growth. For large nuclei densities, the grains impinge before developing any instabilities and remain globular. For lower nuclei densities, instabilities at the solid/liquid interface can develop into dendritic branches, resulting in a mushy grain (Figure 2). Both globular and dendritic microstructures can be observed in

equiaxed castings, and it is the aim of the modeling to predict the occurrence of either structure and the corresponding distribution of secondary phases. Nucleation and growth are influenced by the local cooling conditions, which are modeled using standard heat-flow analyses on the scale of the casting. In the presence of convection, the following effects also need to be considered in modeling on the microscopic scale:
- Fragmentation of dendrites
- Drag forces between equiaxed grains and the liquid
- Convective transport of the rejected solute from the grain into the undercooled melt during growth (or from the superheated melt during remelting)
- Convective influences on dendrite tip growth

For modeling on the macroscopic scale, the following additional effects must be considered.
- Rheological behavior of the melt laden with equiaxed grains
- Buoyancy-induced or forced flow of the melt
- Transport of free equiaxed grains
- Convective heat transport
- Advection and redistribution of solutes by liquid and solid motion

As described below, all of the above effects can be included in a self-consistent model if a multiphase/-scale approach and volume averaging are used. The multiphase approach is inspired by the work of Rappaz and Thevoz[4] and serves to distinguish between different microscopic length scales in equiaxed dendritic solidification. As shown in Figure 2, a hypothetical envelope is drawn around a dendritic grain in order to separate the interdendritic liquid inside the envelope from the extradendritic liquid outside of it. The interdendritic liquid is, thus, associated with a length scale of the order of the secondary dendrite arm spacing, while the extradendritic liquid experiences a length scale that is related to the grain density. For a globulitic grain, the interdendritic liquid does not exist, and the internal solid fraction ε_{si} is equal to unity. The multiphase approach thus allows for the modeling of phenomena as disparate as back-diffusion, coarsen-

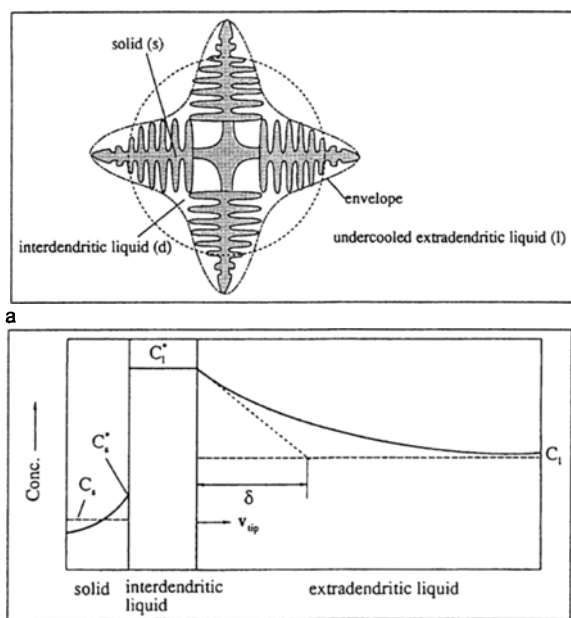Figure 1. A schematic of an equiaxed solidification system.

a

b

Figure 2. Schematic of (a) a single equiaxed dendritic grain and (b) the corresponding solute profiles during growth.

ing, dendrite tip growth, solute rejection from the grain, and flow through and around the grains. The combination of these effects could not be modeled if the grains were considered simply as equivalent solid spheres. Note that the temperature can readily be assumed uniform at the scale of the grain in Figure 2.

FRAGMENTATION

In the absence of convection, a number of empirical nucleation models have been used to calculate the generation rate $\dot{n}_{nucleation}$ of equiaxed grains.[2,3] No model exists to calculate the grain generation rate due to fragmentation of dendrites in the presence of melt flow, $\dot{n}_{fragmentation}$, although a number of relevant experiments have recently been performed.[5,6] It is beyond the scope of this article to discuss the many intricate physical phenomena associated with fragmentation, but this topic likely represents the most significant gap in modeling solidification with convection.

Grain generation rates are used in the following conservation equation for calculating the local grain density n.

$$\frac{\partial n}{\partial t} + \nabla \cdot (v_s n) =$$

$$\dot{n}_{nucleation} + \dot{n}_{fragmentation} - \dot{n}_{remelting} \quad (1)$$

where $\dot{n}_{remelting}$ is the death rate of grains due to complete remelting. The second term on the left side accounts for redistribution of grains due to their motion (with a velocity v_s).

INTERFACIAL DRAG

Knowledge of the interfacial drag between equiaxed grains and the melt is important for calculating their relative motion. For isolated small nuclei and globulitic grains, the well-known Stokes' law can be expected to be appropriate. For dendritic grains, there can be flow of liquid through and around a grain. The situation is further complicated by the presence of other grains. In the limit of packed grains, all of the flow must be through the dendritic structure of the grains. In this case, a permeability associated with Darcy's law is typically used to characterize the drag.

The drag of single equiaxed dendrites was recently measured using both plastic models[7] and the transparent model alloys NH_4Cl-H_2O and succinonitrile (SCN)-acetone.[8,9] For the transparent model alloys, the apparatus consisted of a dendrite generator above a temperature-controlled column. The melt in the column was kept at the liquidus temperature in order to observe the fall of a dendrite of constant size. Based on the measurements, a theory[10] was developed that correlates the drag coefficient in terms of its Reynolds number, the sphericity of the dendrite envelope, and the internal permeability. It reduces to Stokes' law in the limit of a small globular grain. The correlation produced good agreement between measured and calculated settling velocities.

Wang et al.[11] extended this correlation to the case of multiple equiaxed grains, including the packed bed regime (where it reduces to the permeability). It was found that for extradendritic liquid fractions above 0.5, the interdendritic liquid is nearly immobilized (relative to the solid) and all flow is around the dendrite envelope. Good agreement was found between the general drag correlation and previous permeability measurements in metallic-alloy equiaxed mushy zones.[12]
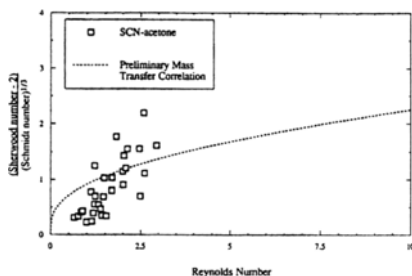

Figure 3. A preliminary correlation of measured Sherwood numbers (dimensionless mass transfer coefficients) with Reynolds number for growth of single equiaxed grains settling in an undercooled melt.
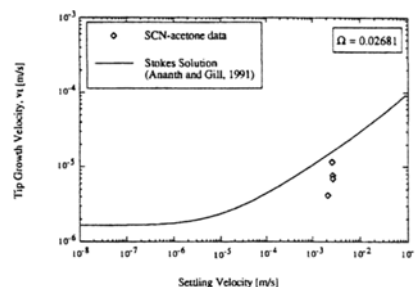

Figure 4. Measured tip growth velocities of single equiaxed grains settling in an undercooled melt and comparison with the Stokes solution of Ananth and Gill.[17]

SOLUTE TRANSPORT

The interdendritic liquid inside the fine dendritic structure of an equiaxed grain can safely be assumed solutely well mixed and at the liquidus concentration C_l^*, corresponding to the local temperature. On the other hand, the transport (by diffusion or convection) of the rejected solute from the envelope into the constitutionally undercooled extradendritic liquid is of critical importance. This transport mainly determines the internal solid fraction of an equiaxed grain. The rate of solute transport from a grain can be characterized by a diffusion length δ (Figure 2). During steady growth of an isolated grain, Rappaz and Thevoz[4] showed that in the limit of purely diffusional transport, δ is given by

$$\delta = D_l/v_t \quad (2)$$

where D_l is the liquid mass diffusivity and v_t is the outward velocity of the envelope that can be taken as the dendrite tip speed. A solute balance leads to the following simple expression for the internal solid fraction of an isolated grain

$$\varepsilon_{si} = \Omega = \frac{C_l^* - C_l}{C_l^*(1-k)} \quad (3)$$

where Ω is the dimensionless solutal undercooling, C_l is the concentration of the melt away from the grain, and k is the partition coefficient.

In the presence of convection, the diffusion length δ can be associated with a convective mass transfer coefficient h_m through

$$h_m = D_l/\delta \quad (4)$$

Then, a solute balance (assuming an immobilized interdendritic liquid) leads to

$$\varepsilon_{si} = (\frac{h_m}{v_t})\Omega \quad (5)$$

In general, $h_m > v_t$ because convection enhances the solute transport away from the grain, resulting in a higher internal solid fraction compared to diffusion. In the limit of no convection, $h_m = v_t$. Note, however, that the dendrite tip speed in
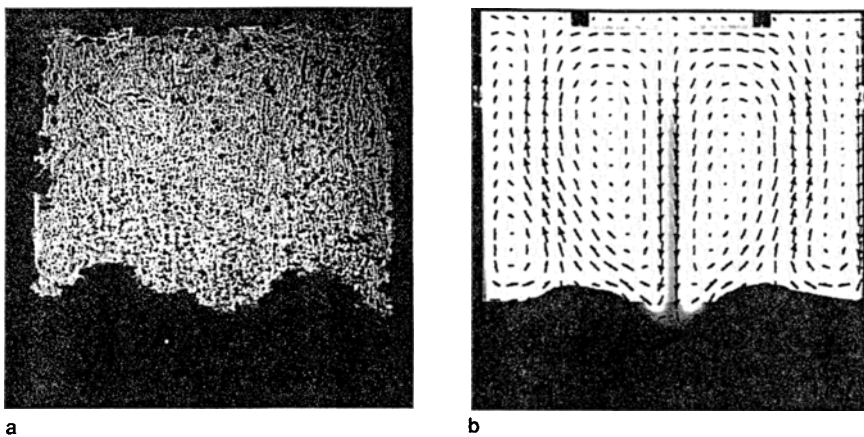
a

b

Figure 5. A comparison of model predictions with NH$_4$Cl-H$_2$O experiments showing (a) a shadowgraph image and (b) the predicted solid fraction field (white = ε_s < 0.1%, black = ε_s > 1%, and continuous gray scale = 0.1% < ε_s < 1%) and liquid velocity vectors ($|v|_{max}$ = 1.7 cm/s).

the presence of convection is much higher than in the diffusion case.

The convective mass transfer coefficient was recently measured using the same apparatus as for the drag coefficient measurements and the transparent model alloys NH$_4$Cl-H$_2$O and SCN-acetone.[9,13] The only difference from the drag coefficient measurements was that the melt in the column was kept at a temperature below the equilibrium liquidus temperature. Hence, an equiaxed grain grows as it settles in the column. The convective mass transfer coefficient h$_m$ can then, in principle, be determined from Equation 5 by measuring the dendrite tip speed v$_t$ and the internal solid fraction ε_{si} for a given undercooling, Ω. Because ε_{si} cannot be measured directly, it is backed out from the drag coefficient correlation[10] by measuring the settling velocity. Finally, the convective mass transfer coefficient was correlated in terms of a Sherwood number using a mass-momentum transfer analogy.[14] The correlation produced only fair agreement with the SCN-acetone measurements (Figure 3), and further research is required. An extension of the correlation to multiple-equiaxed crystals is proposed in Reference 15.

DENDRITE TIP GROWTH

For typical relative velocities between a settling equiaxed grain and the melt, the dendrite tip speed, which is important for determining the grain envelope evolution, can be several times higher than that for purely diffusional growth. While there are theories available to calculate the tip speed (and radius) as a function of the undercooling in quiescent melts,[16] little is known about the influence of convection.

Using the same apparatus and transparent model alloys used for the determination of the drag and mass-transfer coefficients, the dendrite tip velocities were measured for single equiaxed grains settling in a column containing an undercooled melt. The measured tip

velocities as a function of the settling velocity for a given undercooling shown in Figure 4 are for the SCN-acetone alloy. Also, plotted is a prediction based on the Stokes solution of Ananth and Gill.[17] This solution was derived for a uniform flow approaching a single tip parallel to the growth direction. The difference between the experimental data and the theory can be attributed to the presence of a more complicated flow field near the multiple tips of an equiaxed crystal in the experiments. For the present settling velocities, the tip speed can be up to an order of magnitude higher than for purely diffusional growth. More experiments and new theories are clearly needed.

RHEOLOGICAL PROPERTIES OF THE EQUIAXED GRAIN/MELT MIXTURE

Knowledge of the rheological properties is important for calculating the slurry-like flow of equiaxed grains suspended in the melt. Before packing, this slurry may be approximated as a Newtonian fluid having a certain mix-
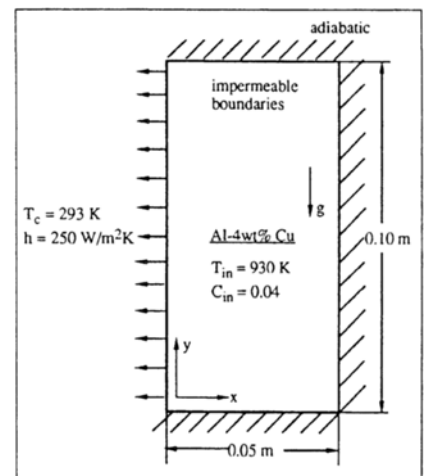

Figure 6. A schematic of the physical system used in the simulation of equiaxed solidification of Al-4Cu.

ture viscosity μ_{mix}. Depending on the volume fraction of grains, ε_g, two limiting cases can be identified. For $\varepsilon_g \to 0$ (small nuclei), the mixture behaves like a dilute suspension of spheres for which Einstein derived μ_{mix} = (1 + 2.5 ε_g)μ_l where μ_l is the liquid viscosity. For the grain fraction approaching the packing limit, ε_g^c, the grains impinge and the solid phase becomes rigid and coherent, so that $\mu_{mix} \to \infty$.

A relation for nonsolidifying mixtures that encompasses both limits has been proposed by Krieger[18] as

$$\mu_{mix} = \varepsilon_g \mu_s + (1-\varepsilon_g)\mu_l =$$
$$\mu_l(1-\varepsilon_g / \varepsilon_g^c)^{-2.5\varepsilon_g^c} \qquad (6)$$

Although Equation 6 was derived for equal solid and liquid velocities, it may be used to calculate an effective solid viscosity μ_s in the case that separate momentum equations are solved for the two phases.

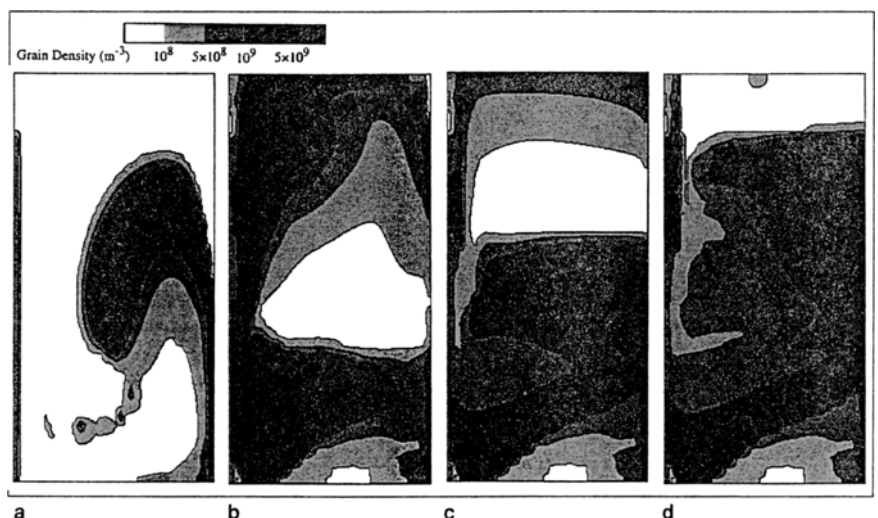In modeling equiaxed solidification, the above viscosity relation should be

Figure 7. The evolution of the grain density for solidification of Al-4Cu (n$_0$ = 10^{9}m^{-3}) when (a) t = 10 s, (b) t = 30 s, (c) t = 50 s, and (d) t =100 s.

based on the grain volume fraction ε_g instead of the solid fraction $\varepsilon_s = \varepsilon_g \times \varepsilon_{si}$. The coherency grain fraction ε_g^c can be taken equal to about 0.5 to 0.6 for both globular and dendritic grains. For globular grains ($\varepsilon_{si} = 1$) that may be present in highly grain-refined castings, the grain fraction coincides with the solid fraction. However, for dendritic grains ($\varepsilon_{si} < 1$), the solid fraction is lower than the grain fraction. Coherency solid fractions as low as 15 percent have been measured.[19] Experiments for concentrated suspensions of equiaxed grains are needed to verify Equation 6 and also to investigate deformations of the mush near and above the coherency point.

THE MULTIPHASE MODEL

The various physical phenomena described have been incorporated in a so-called multiphase model.[15,20] This model consists of averaged (macroscopic) mass, momentum, energy, and species conservation equations for each phase (solid, interdendritic liquid, and extradendritic liquid) together with interfacial balances. The general approach has been outlined in a previous article in *JOM*.[21] There are several additional supplementary relations needed in the model beyond those discussed here, and the reader is referred to Reference 15 for a complete description.

Comparison of the Model Predictions with NH$_4$Cl-H$_2$O Experiments

Some limited validation of the model has been provided by Beckermann and Wang[22] through comparison of model predictions with NH$_4$Cl-H$_2$O experiments. The test cell used in the experi-
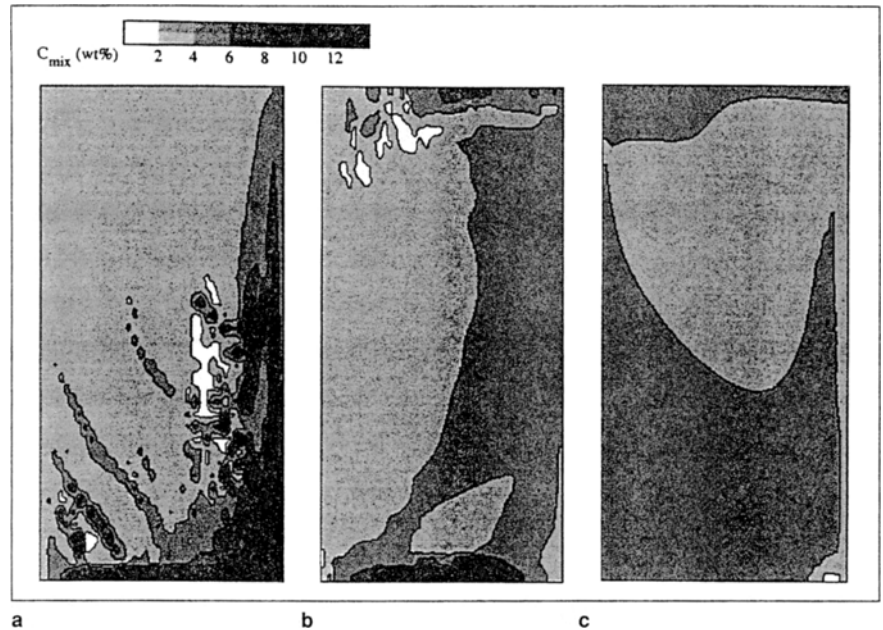
Figure 9. Final macrosegregation patterns for the equiaxed solidification of Al-4Cu with (a) stationary solid ($n_0 = 10^9 \mathrm{m}^{-3}$), (b) moving solid ($n_0 = 10^9 \mathrm{m}^{-3}$), and (c) moving solid ($n_0 = 10^{11} \mathrm{m}^{-3}$).

ments consists of a square enclosure surrounded on four sides by heat exchangers through which a temperature-regulated coolant was circulated. Initially, the enclosure contained a NH$_4$Cl-70H$_2$O (weight percent) solution slightly above the liquidus temperature. After initiation of cooling, melt convection and (with some delay) equiaxed solidification commenced. Density gradients were visualized using a shadowgraph system, and internal cell temperatures were measured using small thermocouples.

A representative comparison of measured and predicted results at an intermediate time is shown in Figure 5. There appears to be good agreement between the measured and predicted extent and shape of the bed of sedimented NH$_4$Cl crystal at the bottom of the enclosure. Considering that this bed is the result of complex growth, melt convection, and solid transport processes, even this limited comparison can be viewed as an encouraging result. Interestingly, it was found that the free equiaxed NH$_4$Cl crystals had an internal solid fraction of the order of only five percent, emphasizing the need to distinguish between the grain and solid volume fractions in the dendritic case. The most critical uncertainty was found to be the modeling of the generation of equiaxed

crystals by fragmentation (the grain density n_0 was adjusted in the model to achieve realistic crystal sizes). Future research will be aimed at resolving this issue.

Application to Solidification of an Al-4Cu Alloy

Illustrative numerical results have been obtained[23] for equiaxed solidification of an Al-4Cu (weight percent) alloy in a two-dimensional rectangular cavity (Figure 6). The left vertical wall is subject to convective cooling, while all other walls are adiabatic. In the Al-Cu system, the melt density increases with increasing copper concentration and decreasing temperature, so that the thermal and solutal buoyancy forces in and near the mushy zone augment each other. The solid density is generally greater than the liquid density. Hence, grain sedimentation is expected in solidification.

A series of predicted grain density fields for a simulation where the initial nuclei density n_0 was set to $10^9 \mathrm{m}^{-3}$ is shown in Figure 7 at various times during solidification. Initially (Figure 7a), a stream of small grains is swept into the central part of the cavity. At t = 30 s (Figure 7b), the grains lifted by the liquid flow along the right wall begin to resettle near the left wall. The settling effect is more evident in Figure 7c (t = 50 s), which shows a pronounced vertical variation in the grain density. The interface between the lower packing region and the upper nearly solid-free liquid region coincides with a relatively sharp vertical gradient in the grain density. At t = 100 s (Figure 7d), this interface is shifted upward as the sediment bed increased in height.
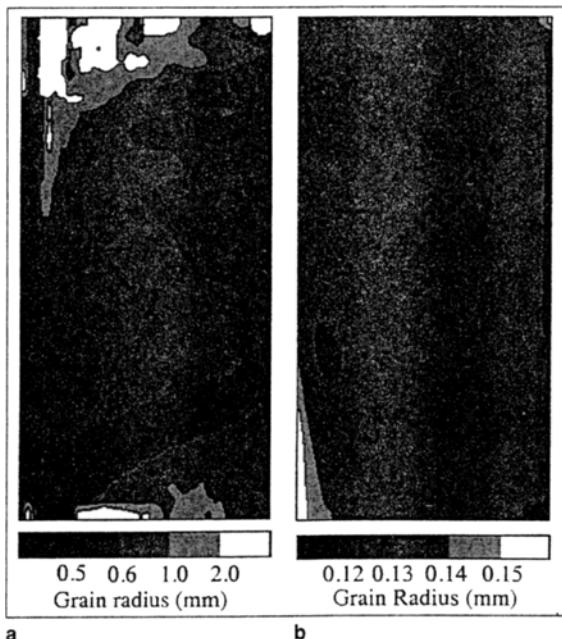
The final grain size distribution for

Figure 8. Final grain size distribution for equiaxed solidification of Al-4Cu for (a) $n_0 = 10^9 \mathrm{m}^{-3}$ and (b) $n_0 = 10^{11} \mathrm{m}^{-3}$.

this simulation is shown in Figure 8a. Note that in the absence of solid transport, the grain size (i.e., radius) would be uniformly equal to 0.62 mm corresponding to $n_0 = 10^9 m^{-3}$. The top zone of larger grains (~2 mm) can be directly attributed to the sedimentation effect.

Shown in Figure 8b is the final grain size distribution for another simulation, where the initial nuclei density n_0 was increased to $10^{11} m^{-3}$, which can correspond to a grain-refined casting. The resulting overall smaller grain size in this case has a profound effect on the solidification and transport phenomena; the equiaxed crystals tend to grow in a more globular fashion, and there is less relative motion between the liquid and solid phases due to the larger interfacial drag. One of the consequences is a much more uniform grain size distribution when $n_0 = 10^{11} m^{-3}$ (Figure 8b) than for $10^9 m^{-3}$ (Figure 8a).

The effects of solid transport and different grain sizes on macrosegregation are illustrated in Figure 9 by comparing the results of three different simulations. Figure 9a is for a case where the solid is assumed to be stationary at all times, but with thermosolutal melt covection and $n_0 = 10^9 m^{-3}$. The most prominent macrosegregation feature is the channel segregates. The channels are oriented downward due to the downward direction of the solutal buoyancy forces in the Al-Cu alloy. Also, a highly segregated copper-rich region exists at the bottom of the cavity and near the right wall due to the advection of solute-rich liquid during solidification. This macrosegregation pattern should be contrasted with Figures 9b and 9c, which correspond to a

moving solid phase (until packing) and $n_0 = 10^9 m^{-3}$ and $10^{11} m^{-3}$, respectively. In general, the macrosegregation is much less severe than in Figure 9a, and no channel segregates are predicted. Because macrosegregation is due to relative motion between the solid and liquid phases, solid transport can be expected to reduce macrosegregation in the present system. However, in cases where the solute-rich liquid is less dense and the solute-poor solid is more dense than the initial melt (e.g., as for hypoeutectic Pb-Sn alloys), a counter current liquid-solid flow would result, causing very strong macrosegregation. Comparing Figures 9b and 9c, it can be seen that a finer grain size in the Al-Cu system results not only in a more uniform grain size distribution, as observed in Figure 8, but also reduces the extent of macrosegregation (due to less relative phase motion).

ACKNOWLEDGEMENTS

References

1. D.G. McCartney, "Grain Refining of Aluminum and Its Alloys Using Inoculants," *Int. Mat. Rev.*, 34 (1989), pp. 247–260.
2. M. Rappaz, "Modeling of Microstructure Formation in Solidification Processes," *Int. Mat. Rev.*, 34 (1989), pp. 93–123.
3. D.M. Stefanescu, "Critical Review of the Second Generation of Solidification Models for Castings: Macro Transport—Transformation," *Modeling of Casting, Welding and Advanced Solidification Processes VI* (Warrendale, PA: TMS, 1993), pp. 3–20.
4. M. Rappaz and Ph. Thevoz, "Solute Diffusion Model for Equiaxed Dendritic Growth," *Acta Metall.*, 35 (1987), pp. 1487–1497.
5. C.J. Paradies et al., "The Effect of Flow Interactions with Dendritic Mushy Zones: A Model Experiment," *Modeling of Casting, Welding and Advanced Solidification Processes VI* (Warrendale, PA: TMS, 1993), pp. 309–316.
6. J.A. Ortega and J. Beech, "Influence of Forced Convection on the Macrostructure of Aluminium and Aluminium-Copper Castings," *Modeling of Castiing VII* (Warrendale, PA:

TMS, 1995), pp. 117–125.
7. R. Zakhem, P.D. Weidman, and H.C. de Groh, III, "On the Drag of Model Dendrite Fragments at Low Reynolds Number," *Metall. Trans. A*, 23A (1992), pp. 2169–2181.
8. S. Ahuja, M.S. thesis, University of Iowa, 1992.
9. R. Anaparti, M.S. thesis, University of Iowa, 1996.
10. H.C. de Groh III, et al., "Calculation of Dendrite Settling Velocity Using a Porous Envelope," *Metall. Trans. B*, 24B (1993), pp. 749–753.
11. C.Y. Wang et al., "Multiparticle Interfacial Drag in Equiaxed Solidification," *Metall. Mater. Trans. B.*, 26B (1995), pp. 111–119.
12. D.R. Poirier and S. Ganesan, "Permeability for Flow of Interdendritic Liquid in Equiaxial Structures," *Mater. Sci. and Eng.*, A157 (1992), pp. 113–123.
13. A. Ramani, M.S. thesis, University of Iowa, 1995.
14. P.A. Agarwal, "Transport Phenomena in Multi-Particle Systems—II. Particle-Fluid Heat and Mass Transfer," *Chem. Sci. Eng.*, 43 (1988), pp. 2501–2510.
15. C.Y. Wang and C. Beckermann, "Equiaxed Dendritic Solidification with Convection. Part I. Multiscale/Multiphase Modeling," *Metall. Mat. Trans. A*, 27A (1996), pp. 2754–2764.
16. W. Kurz and D.J. Fisher, *Fundamentals of Solidification* (Aedermannsdorf, Switzerland: Trans Tech, 1989).
17. R. Ananth and W.N. Gill, "Self-Consistent Theory of Dendritic Growth with Convection," *J. Crystal Growth*, 108 (1991), pp. 173–189.
18. I.M. Krieger, "Rheology of Monodisperse Lattices," *Adv. Colloid Interf. Sci.* B (1972), pp. 111–136.
19. L. Amberg, G. Chai, and L. Backerud, "Determination of Dendritic Coherency in Solidifying Melts by Rheological Measurements," *Mater. Sci. Eng.*, A173 (1993), pp. 101–103.
20. C. Beckermann and C.Y. Wang, "Multiphase/-scale Modeling of Alloy Solidification," *Annual Review of Heat Transfer VI* (New York: Begell House, 1995), pp. 115–198.
21. C. Beckermann and C.Y. Wang, "Incorporation of Interfacial Phenomena in Solidification Models," *JOM*, 46 (1994), pp. 42–47.
22. C. Beckermann and C. Y. Wang, "Equiaxed Dendritic Solidification with Convection, Part III. Comparisons with NH_4Cl-H_2O Experiments," *Metall. Mat. Trans. A*, 27A (1996), pp. 2784–2795.
23. C.Y. Wang and C. Beckermann, "Equiaxed Dendritic Solidification with Convection, Part II. Numerical Simulations for an Al-4 Wt Pct Cu Alloy," *Metall. Mat. Trans. A*, 27A (1996), pp. 2765–2783.

ABOUT THE AUTHOR

C. Beckermann earned his Ph.D. in mechanical engineering at Purdue University in 1987. He is currently a professor at the Unviersity of Iowa. He is also a member of TMS.

For more information, contact C. Beckermann, Department of Mechanical Engineering, 2212 Engineering Building, Iowa City, Iowa 52242; (319) 335-5681; fax (319) 335-5669; e-mail becker@icaen.uiowa.edu.

SUBMITTING PAPERS TO *JOM*

Author Kit

Potential authors should formally notify the editorial staff of their publishing intent by submitting a 300-word abstract, probable title, and a brief biographical sketch. Anyone wishing to publish in *JOM* should follow the guidelines established in the *JOM* Author Kit. This material, supplied on request, features detailed information on communication, manuscript preparation, and publication procedure. Articles are scheduled according to the Technical Emphasis Calendar, developed with members of the *JOM* Advisory Committee, who assist the editorial staff in selecting papers and arranging for qualified review.

Scheduling

Publication deadlines allow approximately 12–14 weeks for review, editing, proofing, typesetting, design, and printing. Since each issue carries a number of articles that must fit within topical and size constraints, author cooperation is expected. Minor delays can be very disruptive to the production process, and the editors should be quickly notified when problems arise.

Manuscript Preparation

In brief, a correctly prepared manuscript is typed, double spaced, on 8.5 × 11 inch (22 × 28 cm) paper. Manuscripts (text and graphics) prepared on computer diskettes or submitted by e-mail are not only welcome, but encouraged. The editorial office can handle a variety of formats. Papers must include: a title, a byline, a summary, an introduction, appropriate subheads, a conclusion, author biographies, references, glossy prints and/or high-quality artwork, and the address, telephone, and fax numbers of the designated contact author. All units *must* be in metric; SI is preferred.

To Receive an Author Kit, Call or Write:

JOM, 420 Commonwealth Drive, Warrendale, Pennsylvania 15086; telephone (412) 776-9000, ext. 224; fax (412) 776-3770; e-mail jom@tms.org

James J. Robinson, Editor